2023 IEEE/ASME International Conference on Advanced Intelligent Mechatronics (AIM)
June 28-30, 2023. Seattle, Washington, USA

A Novel Series Elastic Actuator with Variable Stiffness

Chao Wang, Zhenhong Li, Bo Sheng, Manoj Sivan, Zhi-Qiang Zhang, Gu-Qiang Li, and Sheng Quan Xie

***Abstract*—Recent studies proposed various robotic joint actuators with variable stiffness to enhance the physical human-robot interaction. However, these actuators were designed on the basis of the planar dynamic models, which limited the optimization of the structure and size of the actuator. This paper proposes a novel concept of incorporating a three-dimensional dynamic model in the design of variable stiffness actuators (VSAs), enabling more compact design of VSAs. A design of VSA is presented according to the proposed concept. The output torque and stiffness are modelled based on the dynamics of the actuator to identify the torque-deflection and stiffness-deflection relations. Simulation is conducted to analyse the dynamic behaviour of the proposed VSA. A prototype is created to evaluate the performance of the proposed VSA through experiments. The simulation results indicate that the proposed concept provides a reasonable principle for stiffness variation of VSAs. The torque estimation accuracy of the model is investigated by comparing the estimated torque with the torque measured by a torque sensor. The result illustrates that the model can estimate the output torque of the proposed VSA accurately. The dynamic behaviour of the proposed VSA is tested through the free vibration test.**

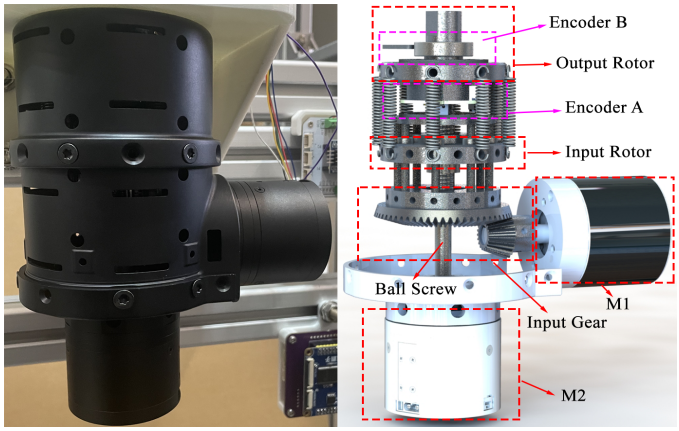

Fig. 1. Prototype (left) and structure (right) of the proposed VSA. M1 and M2 are the DC motors controlling the main driver and spring preload, respectively. Encoder A measures the deflection angle between the input and output rotor. Encoder B measures the displacement of output rotor.

I. INTRODUCTION

Compliance plays an important role in the safety of physical human-robot interaction (pHRI) [1], [2]. To mitigate the risk of injury to users, robotic actuators has introduced compliant component with inherent compliance to ensure the intrinsic safety of pHRI [3]–[5]. Most of the compliant actuators are designed with fixed stiffness depending on a pre-determined working condition. However, the increased complexity of pHRI requires the stiffness of actuators to be adjustable to improve the adaptability and robustness, enabling the actuator to respond more effectively to different pHRI scenarios.

Recent studies proposed various designs for variable stiffness actuators (VSAs). According to their structure, they can be classified into two categories: antagonistic-type [6]–[8] and series-type VSAs. Antagonistic-type VSAs are designed to work similarly to the human body, using two opposing drivers to change the stiffness and output torque. This design allows for easy compensation of potential displacement between the joint and the actuator in cable-driven systems, which can be a common issue in robotics applications. However, this type of VSA requires complex control algorithms to function properly and consumes additional energy compared to other designs. In contrast, series-type VSAs typically use two separate motors for joint positioning and stiffness regulation [9], making them easier to control and more energy-efficient.

The stiffness variation mechanisms of series-type VSAs can be grouped as follows: 1) Changing the transmission ratio between the output and the elastic element, e.g., AWAS-II [10], [11] and [12]; 2) Changing the preload of the elastic element, e.g., MACCEPA 2.0 [13], [14], and LVSA [15]; 3) Changing the property of the elastic element, e.g., S^3VSA [16], pneumatic VSAs [17], [18], and [19]. VSAs using variable leverage mechanism adjust the stiffness by changing the force point and moment arm of the spring force, leading to a direct change of torque produced by the passive motion of the output without reducing energy storage capacity. However, the transmission ratio change mechanism is usually bulky, complex, and potentially less efficient. Changing spring preload is simple and easy to control but may reduce energy storage capacity. Changing elastic element properties is an interesting way to change stiffness, but the actuators based on the previous two principles have better performance than the state-of-art actuators adjusting stiffness by changing elastic element properties. Recent studies have proposed reconfigurability for stiffness variation, but these actuators still can be categorized into the first two groups [14], [20], [21].

The stiffness of a system can be adjusted by changing the transmission ratio and preload of an elastic element, which in turn affects the two factors that determine a torque: moment arm and force. Previous studies have simplified the dynamics of both antagonistic-type and series-type actuators as planar models because both the force and moment arm vectors reside in two parallel planes [21]–[26]. However, this limits the optimization of structure, size, and the placement of other components. Expanding the force and moment arm vectors to three-dimensional space may provide opportunities for optimizing actuator design.

In this paper, we propose a novel principle of modelling and designing a VSA in three-dimensional space. Then, a VSA is designed based on the proposed principle. The output torque and stiffness are controlled by two independent DC motors, respectively. Eight springs are used to provide compliance for

the actuator. A dynamic model is established to identify the torque-deflection and stiffness-deflection relations. Simulation is conducted to analyse the proposed principle of stiffness variation. Then, a prototype of the proposed VSA is created to test the performance. The results reveal that the proposed principle is an effective way of stiffness variation for the VSA, and the proposed model can estimate the output torque of the actuator with promising accuracy.

II. DESIGN

A. Working Principle

Fig. 2 (a) shows a widely used structure of VSAs (both for VSAs adjust stiffness by changing transmission ratio and preload). This structure requires the design of the VSA leave enough space for the output rotor and elastic element. As a result, the dimensions of the actuator along this direction need to be bigger to increase the stiffness and output torque. In this study, a novel 3-D dynamics model is established to support the design of the VSA.

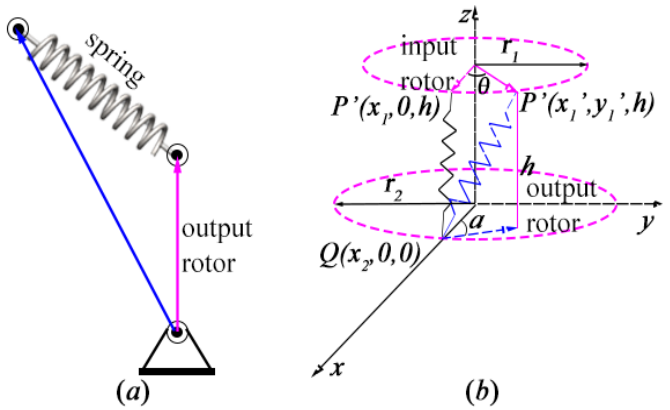

Fig. 2. (a). Working principle of the VSAs proposed in the previous studies based on the planar dynamic model. (b). Working principle of the VSA proposed in this study.

Fig. 2 (b) shows the structure of the dynamics model. There are two rotors coupled with springs, which are the input and output rotors. The projection of spring force on the output rotor is along the radial direction of the output rotor when at the initial position, thereby the output torque is zero. The spring force produces torque along the z-axis with the passive movement of output rotor, and the value of the output torque is related to physical properties of the springs. Change of the distance between the two rotors of the actuator changes the preload of springs which adjusts the stiffness of the actuator. Besides, the stiffness of the actuator can also be adjusted by reconfiguring the number and stiffness of the springs.

B. Mechanical Structure

The mechanical design of the proposed VSA is shown in Fig. 1. The actuator has two units: main driver unit and stiffness adjuster unit. The main driver unit controls the deflection angle between the input and output rotor to control the output torque. The stiffness adjuster unit controls the ball screw to adjust the position of the input rotor which lead to the change of spring preload. The position of the input gear is fixed. As shown in Fig. 3, the ball screw nut is bonded together with the input rotor. The input gear is rigidly connected with eight bars (linear slider rail) which is coupled with the input rotor through eight linear sliders. Therefore, the rotation of the ball screw changes the position of the input rotor along the z-axis, and the deflection of input gear drive causes the same deflection on the input rotor. Consequently, the rotary motion and the displacement along the z-axis of the input rotor (stiffness regulation) is decoupled.

The magnetic ring is immovably connected with the eight bars, thereby the input gear, the eight bars and the magnetic ring is considered as a rigid body. The encoder a is fixedly joined with the output rotor to measure the deflection angle between the magnetic ring and output rotor. Therefore, the outcome of encoder A is considered as the deflection between the input and output rotors. The displacement of the input rotor along the z-axis is determined by the rotary motion of M2. The ball screw is rigidly joined with M2, thereby the deflection angle of the ball screw is considered as the same as M2. Thus, the magnetic encoder in M2 is used to measure the deflection angle of the ball screw.

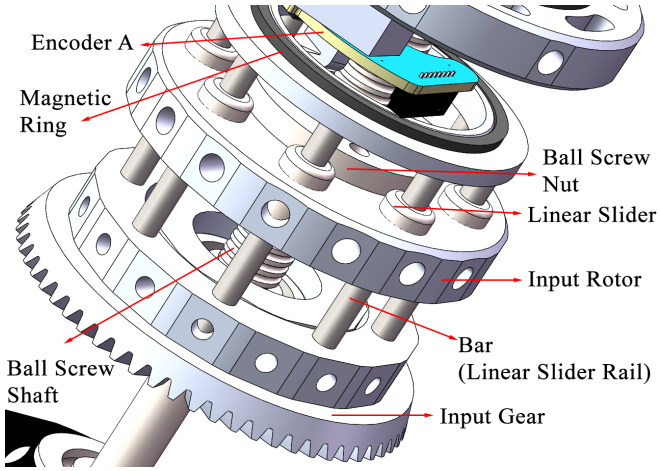

Fig. 3. The connection between the input gear and input rotor.

III. METHODOLOGY

A. Ideal Model of Stiffness

To enable the torque control of the actuator, the torque/deflection and stiffness/deflection relations need to be quantified. Then, the following assumptions are made to facilitate the modelling

Assumption 1. *All the segments in the actuator are considered as rigid except the elastic elements.*

Assumption 2. *The two ends of every elastic element do not change with the deflection.*

The kinematics of the system can be formulated as:

$$\begin{cases} \cos\alpha = \frac{x_1' - x_2}{\sqrt{(x_1'-x_2)^2 + y_1'^2}} \\ x_1' = r_1\cos\theta \\ y_1' = r_1\sin\theta \end{cases} \tag{1}$$

Let the angle between $\overrightarrow{QP'}$ and the xOy plane be β, the following can be found

$$\sin\beta = \frac{h}{\sqrt{(r_1\cos\theta - r_2)^2 + (r_1\sin\theta)^2 + h^2}} \tag{2}$$

Let the original length of the springs be l_0, the spring stretched length can be obtained by

$$\delta l = \sqrt{(r_1\cos\theta - r_2)^2 + (r_1\sin\theta)^2 + h^2} - l_0 \tag{3}$$

then, the spring force can calculated as

$$F_s = k_s\delta l \tag{4}$$

where F_s is the force produced by a single spring, k_s is the stiffness of the springs, h can be obtained by

$$h = h_0 + \Delta h_1 + \Delta h_2 \tag{5}$$

where h_0 is the initial value of h, Δh_1 is the increased value of h caused by the deflection between the plate A and the VSA housing, and Δh_2 is the increased value controlled by the worm gear, they can be computed by

$$\begin{aligned} \Delta h_1 &= \frac{\theta}{2\pi}d \\ \Delta h_2 &= \frac{\lambda}{2\pi}d \end{aligned} \tag{6}$$

where d is the lead of the ball screw, and λ is the deflection angle of the worm gear.

The output torque of the actuator can be computed by

$$\tau = F_{xy}r \tag{7}$$

where F_{xy} is the projection of the spring force on the xOy plane, and r is the moment arm of F_{xy}, which can be calculated by

$$\begin{aligned} r &= r_2\sin\alpha \\ &= \frac{r_1 r_2\sin\theta}{\sqrt{(r_1\cos\theta - r_2)^2 + (r_1\sin\theta)^2}} \end{aligned} \tag{8}$$

and F_{xy} can be calculated by

$$\begin{aligned} F_{xy} &= F_s\cos\beta \\ &= \frac{k_s\delta l\sqrt{(r_1\cos\theta - r_2)^2 + (r_1\sin\theta)^2}}{\sqrt{(r_1\cos\theta - r_2)^2 + (r_1\sin\theta)^2 + h^2}} \end{aligned} \tag{9}$$

The equivalent stiffness of the actuator is defined as

$$\begin{aligned} k_{eq} &= \frac{\delta\tau}{\delta\theta} \\ &= r\frac{\delta F_{xy}}{\delta\theta} + F_{xy}\frac{\delta r}{\delta\theta} \end{aligned} \tag{10}$$

B. Elastic Element Reconfiguration

Beside changing the preload of the elastic elements, the proposed design allows users to replace the elastic elements. Reconfiguring the material and number of the elastic elements will change the upper and lower boundary of the range of stiffness of the actuator, which makes the VSA adaptive for different working conditions. Theoretically, the stiffness range of the proposed VSA is zero to rigid if the plate A and B is coupled through rigid bars. In this study, the actuator is tested with spring stiffness, $k_s = 2500$ N/m.

C. Experimental Setup

To evaluate the performance of the proposed VSA, a prototype is created and tested. The deflection angles, θ and λ are measured through the encoders at 1000 Hz. A torque sensor is utilized to monitor the output torque of the actuator at 250 Hz. Then, there are five groups of test to assess the torque-deflection relation for λ at , $k_s = 2500$ N/m. A basic PID controller is developed to achieve the control of the deflection angles, θ and λ. The whole structure of the controller is shown in Fig. 4.

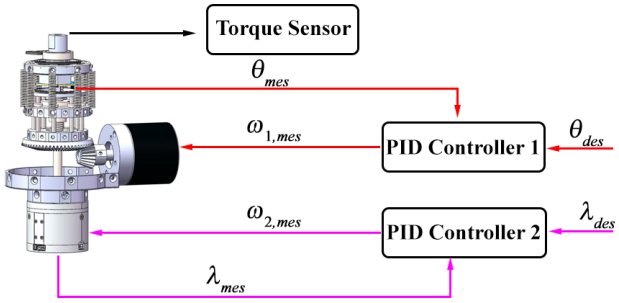

Fig. 4. The structure of the PID controller for the performance test.

IV. Result

Before the prototype test, the performance of the proposed VSA is analysed in simulation to evaluate the proposed working principle of VSA. Figs. 5 and 6 illustrates the theoretical stiffness-deflection and torque-deflection relations for $k_s = 2500$ N/m.

The output torque of the proposed VSA is tested and compared with the estimation of the dynamic model, equation (7). The deflection angle, θ is tested from -18.0° to 18.0° for two different spring preload conditions, λ = λ_1 and λ_2, respectively. During the test, there are four stages: STAGE 1. θ increase from 0.0° to 18.0°; STAGE 2. θ decrease from 18.0° to 0.0°; STAGE 3. θ decrease from 0.0° to -18.0°; STAGE 4. θ increase from -18.0° to 0.0°. Fig. 7 shows the comparison between the torque measured by the torque sensor and estimated by the model, equation (7).

Root-mean-squared error (RMSE) is used to quantify the error between the estimated and measured torque, which is defined as

$$RMSE = \sqrt{\frac{1}{N}\sum_{i=1}^{N}(\tau_i - \widehat{\tau}_i)^2} \tag{11}$$

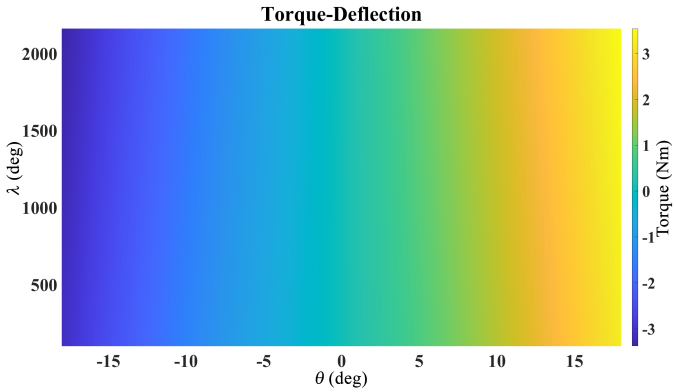

Fig. 5. The torque-deflection relation from simulation for the inherent stiffness of springs, k_s = 2500 N/m.

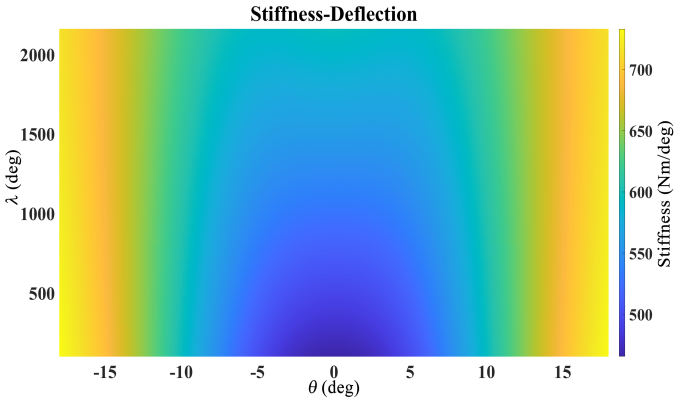

Fig. 6. The stiffness-deflection relation from simulation for the inherent stiffness of springs, k_s = 2500 N/m.

where τ_i is the measured torque, and $\widehat{\tau}_i$ is the torque estimated by the model. Table. I summarizes the RMSE values for both $\lambda = \lambda_1$ and λ_2.

TABLE I
RMSE VALUES FOR QUANTIFY TORQUE ESTIMATION ACCURACY.

k_s (N/m)	$RMSE_{\tau,1}$(Nm)	$RMSE_{\tau,2}$(Nm)
2500	0.1983	0.1088

To evaluate the dynamic behaviour of the VSA, the free vibration tests are conducted for two different spring preload, $\lambda = \lambda_1$ and λ_2, respectively. The pendulum is released from the position θ = 18.0 °. Fig. 8 shows the result of the free vibration tests.

V. DISCUSSION

The simulation results in Figs. 5 illustrates that the proposed actuator generates a torque related to the deflection angle, θ, up to about 3.5 Nm. Fig.6 shows the stiffness-deflection relation which indicates that the stiffness of the actuator can be adjusted through changing λ. Therefore, the proposed structure provides a reasonable principle of stiffness variation for the actuator.

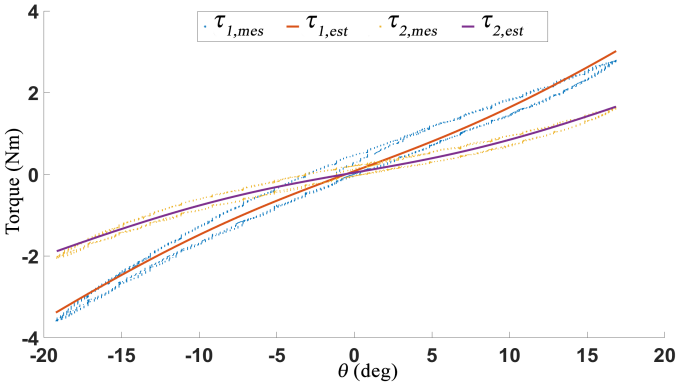

Fig. 7. Comparison between the output torque measured by the torque sensor and estimated by the model, equation (7). $\tau_{1,mes}$ and $\tau_{1,est}$ is the measured and estimated torque for $\lambda = \lambda_1$, and $\tau_{2,mes}$ and $\tau_{2,est}$ is the measured and estimated torque for λ_2, respectively.

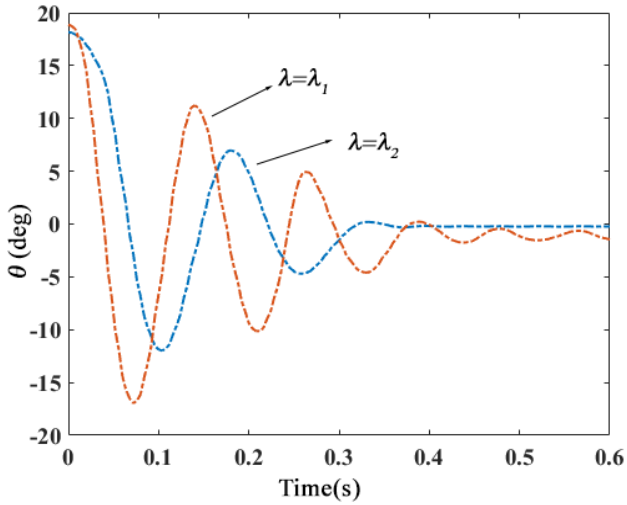

Fig. 8. Time history of free vibration for k_s = 2500 N/m.

Fig. 7 shows the comparison between the output torque measured by torque sensor and estimated by the dynamic model. The results for demonstrates that the proposed model can estimate the output torque of the actuator with promising accuracy for both $\lambda = \lambda_1$, and λ_2. Nevertheless, there is a clear difference between the torque measured from STAGE 1 and 2, and STAGE 3 and 4. Theoretically, the measured torque for STAGE 1 and 2 should be very close, as well as STAGE 3 and 4. The difference shown in Fig. 7 means that there might be a difference in the mechanical structure between STAGE 1 and 2, and STAGE 3 and 4. A possible reason is the bending deformation of spring, which lead non-linearity of spring force. To solve this problem, the coupling mechanism between the spring and the input and output rotor needs to be improved to minimize the bending deformation. Besides, the accuracy of the estimation model for $\lambda = \lambda_2$ is higher than $\lambda = \lambda_2$. The reason can be: 1). the preload of $\lambda = \lambda_1$ is higher than $\lambda = \lambda_2$, which lead to the increase of the friction between the output rotor and the ball screw. 2). the deflection between

the input and output rotor leads to the bending deformation of springs which affects the output torque. To improve the estimation accuracy, the dynamic model needs to be modified to consider more factors influencing the output torque, e.g., friction compensation.

Fig. 8 demonstrates the dynamic behaviour of the VSA in the free vibration test. For $\lambda = \lambda_1$, the amplitude of the position is higher than for $\lambda = \lambda_2$, and the vibration frequency for $\lambda = \lambda_1$ is higher. The reason might be that the increase of spring preload makes the energy stored in the springs higher for the same deflection of θ, thereby the amplitude decay speed is slower.

VI. CONCLUSIONS AND FUTURE WORK

This study proposes a novel concept of stiffness variation mechanism for VSAs. A compact VSA is designed on the basis of the concept. The physical property of the VSA is analysed in simulation, and the results in indicated that the VSA designed on the proposed concept provided a reasonable principle of stiffness variation of VSAs. A prototype of the proposed VSA is made and tested, and a dynamic model is established to estimated the output torque of the VSA based on two deflection angles, θ and λ. The output torque estimation model is validated by comparing the estimated torque with the torque measured by a torque sensor. The results of the comparison illustrated that the proposed model can estimates the output torque with the RMSE value as 0.1983 for $\lambda = \lambda_1$, and 0.1088 for $\lambda = \lambda_2$, respectively. However, the output torque for the same deflection of θ is different when at different stage (STAGE 1 and 2, and STAGE 3 and 4). The future work will be modifying the torque estimation model to achieve a higher torque estimation accuracy, and improve the design of the coupling mechanism between the springs and the input and output rotor to avoid bending deformation of springs.

REFERENCES

[1] A. Calanca and P. Fiorini, "On the Role of Compliance in Force Control," *Intelligent Autonomous Systems 13*, pp. 1243-1255, 2015.

[2] N. Hogan, "Contact and physical interaction," *Annual Review of Control, Robotics, and Autonomous Systems*, vol. 5, no. 1, pp. 179–203, 2022.

[3] B. Zhong, K. Guo, H. Yu, and M. Zhang, "Toward gait symmetry enhancement via a cable-driven exoskeleton powered by series Elastic Actuators," *IEEE Robotics and Automation Letters*, vol. 7, no. 2, pp. 786–793, 2022.

[4] E. Capotorti, E. Trigili, Z. McKinney, E. Peperoni, F. Dell'Agnello, M. Fantozzi, A. Baldoni, D. Marconi, E. Taglione, S. Crea, and N. Vitiello, "A novel torque-controlled hand exoskeleton to decode hand movements combining SEMG and fingers kinematics: A feasibility study," *IEEE Robotics and Automation Letters*, vol. 7, no. 1, pp. 239–246, 2022.

[5] T. Kim, K. Shi, and K. Kong, "A compact transmitted-force-sensing series elastic actuator with optimized planar torsional spring for exoskeletons," *2021 IEEE/ASME International Conference on Advanced Intelligent Mechatronics (AIM)*, 2021.

[6] R. Mengacci, M. Keppler, M. Pfanne, A. Bicchi, and C. Ott, "Elastic structure preserving control for compliant robots driven by agonistic-antagonistic actuators (ESPAA)," *IEEE Robotics and Automation Letters*, vol. 6, no. 2, pp. 879–886, 2021.

[7] W. Roozing, Z. Li, G. A. Medrano-Cerda, D. G. Caldwell, and N. G. Tsagarakis, "Development and control of a compliant asymmetric antagonistic actuator for Energy Efficient Mobility," *IEEE/ASME Transactions on Mechatronics*, vol. 21, no. 2, pp. 1080–1091, 2016.

[8] T. Luong, S. Seo, K. Kim, J. Jeon, F. Yumbla, J. C. Koo, H. R. Choi, and H. Moon, "Realization of a simultaneous position-stiffness controllable antagonistic joint driven by twisted-coiled polymer actuators using model predictive control," *IEEE Access*, vol. 9, pp. 26071–26082, 2021.

[9] S. Wolf, G. Grioli, O. Eiberger, W. Friedl, M. Grebenstein, H. Hoppner, E. Burdet, D. G. Caldwell, R. Carloni, M. G. Catalano, D. Lefeber, S. Stramigioli, N. Tsagarakis, M. Van Damme, R. Van Ham, B. Vanderborght, L. C. Visser, A. Bicchi, and A. Albu-Schaffer, "Variable stiffness actuators: Review on design and components," *IEEE/ASME Transactions on Mechatronics*, vol. 21, no. 5, pp. 2418–2430, 2016.

[10] A. Jafari, N. G. Tsagarakis, B. Vanderborght, and D. G. Caldwell, "A novel actuator with adjustable stiffness (AWAS)," *2010 IEEE/RSJ International Conference on Intelligent Robots and Systems*, 2010.

[11] A. Jafari, N. Tsagarakis and D. Caldwell, "AwAS-II: A new Actuator with Adjustable Stiffness based on the novel principle of adaptable pivot point and variable lever ratio," *2011 IEEE International Conference on Robotics and Automation*, 2011.

[12] Y. Liu, S. Cui, and Y. Sun, "Mechanical design and analysis of a novel variable stiffness actuator with symmetrical pivot adjustment," *Frontiers of Mechanical Engineering*, vol. 16, no. 4, pp. 711–725, 2021.

[13] B. Vanderborght, N. G. Tsagarakis, C. Semini, R. Van Ham and D. G. Caldwell, "MACCEPA 2.0: Adjustable compliant actuator with stiffening characteristic for energy efficient hopping," *2009 IEEE International Conference on Robotics and Automation*, 2009.

[14] Y. Xu, K. Guo, J. Sun, and J. Li, "Design, modeling and control of a reconfigurable variable stiffness actuator," *Mechanical Systems and Signal Processing*, vol. 160, p. 107883, 2021.

[15] C. Wang, B. Sheng, Z. Li, M. Sivan, Z.-Q. Zhang, G.-Q. Li, and S. Q. Xie, "A lightweight series elastic actuator with variable stiffness: Design, modeling, and evaluation," *IEEE/ASME Transactions on Mechatronics*, pp. 1–10, 2023.

[16] Y. Xu, K. Guo, J. Li, and Y. Li, "A novel rotational actuator with variable stiffness using S-shaped springs," *IEEE/ASME Transactions on Mechatronics*, vol. 26, no. 4, pp. 2249–2260, 2021.

[17] L. Miskovic, M. Dezman, and T. Petric, "Pneumatic quasi-passive variable stiffness mechanism for energy storage applications," *IEEE Robotics and Automation Letters*, vol. 7, no. 2, pp. 1705–1712, 2022.

[18] Y. Sun, P. Tang, D. Dong, J. Zheng, X. Chen, and L. Bai, "Modeling and experimental evaluation of a pneumatic variable stiffness actuator," *IEEE/ASME Transactions on Mechatronics*, vol. 27, no. 5, pp. 2462–2473, 2022.

[19] E. Barrett, J. Malzahn, and N. Tsagarakis, "A compliant mechanism with progressive stiffness for robotic actuation," *2021 IEEE/ASME International Conference on Advanced Intelligent Mechatronics (AIM)*, 2021.

[20] Y. Zhu, Q. Wu, B. Chen, D. Xu and Z. Shao, "Design and Evaluation of a Novel Torque-Controllable Variable Stiffness Actuator With Reconfigurability," *IEEE/ASME Transactions on Mechatronics*, vol. 27, no. 1, pp. 292-303, 2022.

[21] X. Li, H. Zhu, W. Lin, W. Chen and K. Low, "Structure-Controlled Variable Stiffness Robotic Joint Based on Multiple Rotary Flexure Hinges," *IEEE Transactions on Industrial Electronics*, vol. 68, no. 12, pp. 12452-12461, 2021.

[22] R. Chaichaowarat, S. Nishimura, and H. I. Krebs, "Design and modeling of a variable-stiffness spring mechanism for impedance modulation in physical human–robot interaction," 2021 IEEE International Conference on Robotics and Automation (ICRA), 2021.

[23] J. Sun, Z. Guo, Y. Zhang, X. Xiao and J. Tan, "A Novel Design of Serial Variable Stiffness Actuator Based on an Archimedean Spiral Relocation Mechanism," *IEEE/ASME Transactions on Mechatronics*, vol. 23, no. 5, pp. 2121-2131, 2018.

[24] K. W. Hollander, T. G. Sugar and D. E. Herring, "Adjustable robotic tendon using a 'Jack Spring'," *9th International Conference on Rehabilitation Robotics*, 2005. pp. 113-118.

[25] Z. Li, W. Chen, J. Zhang, Q. Li, J. Wang, Z. Fang, and G. Yang, "A novel cable-driven antagonistic joint designed with variable stiffness mechanisms," *Mechanism and Machine Theory*, vol. 171, p. 104716, 2022.

[26] Z. Liu, H. Jin, H. Zhang, Y. Liu, Y. Long, X. Liu, and J. Zhao, "A variable stiffness actuator based on second-order lever mechanism and its manipulator integration," *2021 IEEE International Conference on Robotics and Automation (ICRA)*, 2021.